

# **Mathematical Modelling of Engineering Problems**

Vol. 12, No. 9, September, 2025, pp. 2993-3002

Journal homepage: http://iieta.org/journals/mmep

# Analysis of Monocrystalline and Polycrystalline Photovoltaic Efficiency on Dual-Axis Solar Tracker System Based on Internet of Things



Diefa Nasywa Aedelia\* Danar Susilo Wijayanto

Department of Mechanical Engineering Education, Universitas Sebelas Maret, Surakarta 57126, Indonesia

Corresponding Author Email: diefanasywa@student.uns.ac.id

Copyright: ©2025 The authors. This article is published by IIETA and is licensed under the CC BY 4.0 license (http://creativecommons.org/licenses/by/4.0/).

https://doi.org/10.18280/mmep.120904

Received: 12 August 2025 Revised: 17 September 2025 Accepted: 22 September 2025

Available online: 30 September 2025

#### Keywords:

monocrystalline solar panel, polycrystalline solar panel, dual-axis solar tracker, Internet of Things (IoT), energy efficiency, photovoltaic performance, renewable energy

#### **ABSTRACT**

This study analyzes and compares the efficiency of monocrystalline and polycrystalline photovoltaic cells mounted on a dual-axis solar tracker system integrated with Internet of Things (IoT)-based monitoring. The experiment was conducted over 31 consecutive days in July 2025, with data collected daily from 7:00 AM to 5:00 PM. Key parameters measured included sunlight intensity (lux), voltage (V), current (I), power output (P), and energy conversion efficiency. The results demonstrated that the monocrystalline panel achieved an average daily power output of 4.91 W with an efficiency of 16.35%, while the polycrystalline panel recorded 2.22 W and an 7.11% efficiency. The maximum efficiency difference between the two panels was 11.75%, occurring at 11:15 AM, which indicates the superior performance of monocrystalline technology under varying irradiance conditions. Furthermore, a dual-axis solar tracker significantly improved solar energy capture and stabilized power generation by adjusting panel orientation to follow the sun's movement. Integration with IoT enables real-time data acquisition and monitoring, ensuring accurate system performance analysis. These findings highlight the higher efficiency of the monocrystalline panel compared to the polycrystalline panel, and emphasize the crucial role of the dual-axis solar tracker combined with IoT in optimizing the performance of small-scale photovoltaic systems.

### 1. INTRODUCTION

The demand for renewable energy is increasing as fossil fuel resources dwindle and environmental problems escalate. Among various renewable energy sources, solar energy is considered one of the most promising due to its abundant availability, sustainability, and relatively simple conversion technology [1, 2]. Photovoltaic (PV) systems can convert solar radiation into electrical energy, and their performance is influenced by various factors, including the type of panel, environmental conditions, and the mechanism for tracking the sun's position [3-5].

Monocrystalline and polycrystalline solar panels are the two most widely used PV technologies. Monocrystalline solar panels generally have higher efficiency due to their uniform crystal structure, while polycrystalline solar panels are more economical but have lower efficiency, especially under low radiation intensity conditions [6]. The efficiency of solar panels can be further improved by using a solar tracker system, which maintains the optimal angle between the panel and the direction of sunlight. Several studies have reported that the using a dual-axis solar tracker can significantly increase power output compared to static or single-axis systems [3].

In addition, Internet of Things (IoT) technology developments have enabled real-time monitoring and control of PV systems, thereby improving reliability, facilitating data acquisition, and supporting predictive maintenance

capabilities [5]. Integration of IoT with solar trackers provides added value in the form of continuous system performance data, especially in tropical regions where solar radiation intensity varies throughout the day [7].

This study is designed with several objectives, namely to measure the voltage, current, and power output of solar panels along with the sunlight intensity received by the panels in a dual-axis solar tracker system, to analyze the performance of solar panels with dual-axis tracking in maximizing solar energy absorption based on real-time IoT-based monitoring, to compare the energy output of monocrystalline and polycrystalline panels under identical conditions, and to evaluate the accuracy of the IoT-based monitoring system in recording and displaying PV performance data.

This study hypothesizes that monocrystalline solar panels, combined with a dual-axis tracker and IoT-based monitoring, will achieve higher efficiency and more stable performance than polycrystalline panels operating under the same conditions.

This work provides a comprehensive assessment by integrating dual-axis tracking with IoT-based real-time monitoring to evaluate two widely used PV technologies in a tropical climate. By addressing panel characteristics, tracking performance, and monitoring reliability in a single framework, the findings are expected to offer practical insights for enhancing the application of photovoltaic systems in regions with fluctuating solar radiation.

#### 2. LITERATURE REVIEW

Solar energy is an environmentally friendly, renewable source abundantly available in Indonesia [8]. Solar panels, called PV modules, convert sunlight into electrical energy through the photovoltaic effect [9, 10]. There are two common types of PV panels, namely monocrystalline and polycrystalline [11, 12]. Monocrystalline solar panels are made from a single crystal structure and generally provide higher efficiency, while polycrystalline solar panels are made from multiple crystal fragments and are less efficient. The performance of PV panels is strongly affected by sunlight intensity and incidence angle [2, 5, 13].

Solar trackers are devices designed to adjust the orientation of panels to follow the sun's movement [14]. A dual-axis solar tracker can adjust both azimuth and elevation angles, offering higher efficiency than single-axis or fixed systems [15]. Moreover, research in tropical regions indicates that solar trackers reduce the impact of fluctuating irradiance due to cloud coverage [16, 17]. Studies indicate that dual-axis tracking PV systems achieve a 30.4 to 34.6% efficiency improvement compared to simulations of fixed PV systems [15].

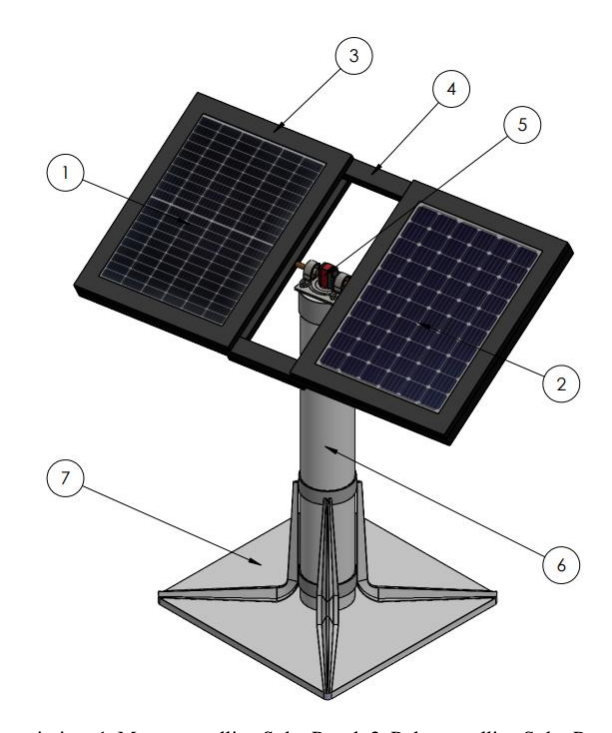
Integration with IoT technology enables real-time monitoring and automated data recording, improving system accuracy and usability [7]. IoT-based PV monitoring systems provide efficient data visualization, remote access, and predictive maintenance capabilities [5, 13]. Several studies have demonstrated that combining IoT with solar trackers improves the reliability of PV systems and simplifies performance evaluation. Recent advances also highlight the role of IoT in enabling adaptive energy management and cloud-based data analytics for PV systems [18].

#### 3. METHODOLOGY

# 3.1 Research method

The research was conducted in Sukoharjo, Central Java, Indonesia, during July 2025. Two solar panels with 18 Wp capacity, one monocrystalline and one polycrystalline, were installed on a dual-axis solar tracker controlled by an Arduino microcontroller. The system was equipped with sensors to measure sunlight intensity, voltage, and current, while power was calculated as  $P = V \times I$ . The data acquisition used PLX-DAQ software for automatic recording in Microsoft Excel, and real-time monitoring was implemented using the Blynk IoT application on smartphones. Measurements were taken every 15 minutes between 7:00 AM until 5:00 PM for 31 consecutive days. Collected data included solar radiation intensity, panel voltage, current, power output, and efficiency calculated from the ratio of electrical power output to solar radiation input.

To ensure reliability, all sensors were calibrated prior to data collection. The voltage and current sensors (INA219) were calibrated against a digital multimeter (accuracy  $\pm 0.5\%$ ), while the BH1750 light sensor was compared with a reference lux meter. Measurement uncertainty was quantified using repeated trials, with the standard deviation reported for each parameter. The combined uncertainty was calculated using the root-sum-square method, and the overall error margin was maintained below 2% for voltage and current, and 3% for light intensity. In addition to the instrumentation setup, the overall design of the dual-axis solar tracker was modeled using SolidWorks software, as illustrated in Figure 1.



Description: 1. Monocrystalline Solar Panel; 2. Polycrystalline Solar Panel; 3. Solar Panel Frame; 4. Solar Panel Bottom Frame; 5. Servo Motor; 6. Support Frame Tube; 7. Base Plate Frame

**Figure 1.** Solar panel design with dual-axis solar tracker system designed using SolidWorks software

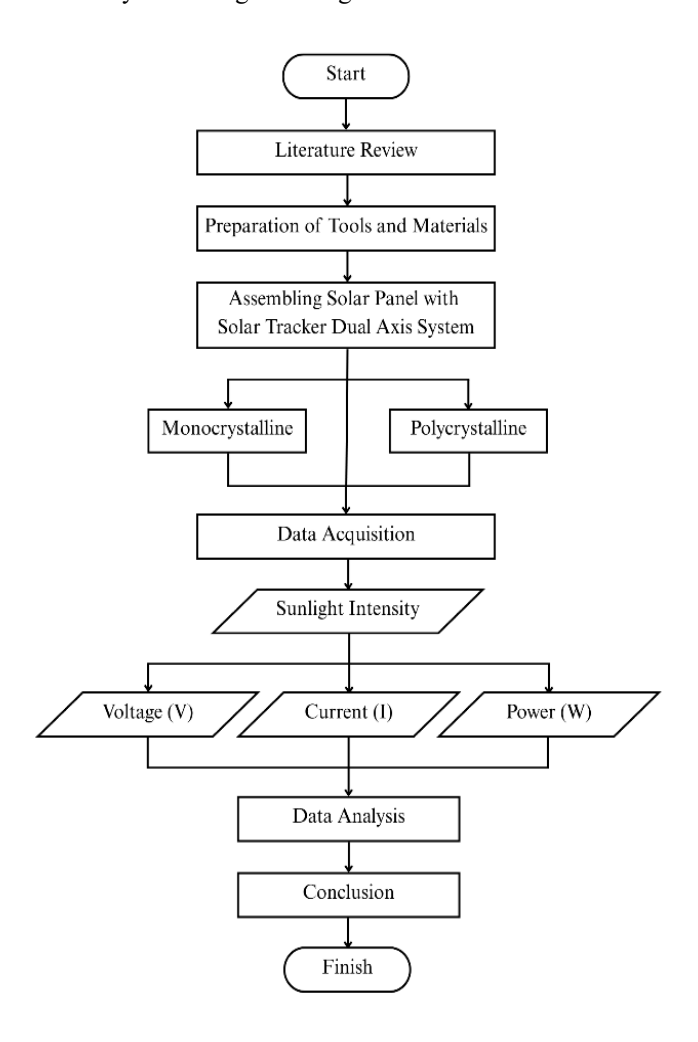


Figure 2. Research flow chart

## 3.2 System design

This study uses a dual-axis solar tracker system based on a microcontroller with integrated IoT technology. Two solar panels of different types, monocrystalline (18 Wp) and polycrystalline (18 Wp), are installed on a sun tracking frame that can move on the azimuth and elevation axes. An Arduino Uno microcontroller is combined with an ESP8266 module for IoT connectivity. At the same time, a Light Dependent Resistor (LDR) sensor is used as a light intensity detector to adjust the panel orientation.

This research began with a literature review on solar energy, solar panel systems, dual-axis solar tracker technology, and IoT-based monitoring, followed by the preparation of tools and materials including monocrystalline and polycrystalline solar panels as well as Arduino-based tracker components equipped with LDR, INA219, and BH1750 sensors. After assembling the system, both panels were installed in parallel on the dual-axis solar tracker and tested simultaneously under direct sunlight for 31 days from 7:00 AM until 5:00 PM. Data collected included sunlight intensity, voltage, current, and electrical power, recorded automatically using PLX-DAQ and monitored in real-time via the Blynk app. The data were

analyzed descriptively to compare the performance of the two panel types, evaluate the effectiveness of the dual-axis tracker, and assess the accuracy of the IoT-based monitoring system, with the research stages illustrated in Figure 2, which presents the research flow chart.

The electrical circuit was designed using the Fritzing application with an Arduino Uno microcontroller as the control center, connected to an LDR sensor for light detection and servo motors for azimuth and elevation movement, allowing the solar panel to follow sunlight automatically. The system integrates an INA219 sensor to measure voltage and current, a BH1750 sensor to monitor light intensity in lux, and an ESP8266 module to transmit real-time data to the Blynk application. At the same time, all data are also automatically recorded via PLX-DAQ. Thus, the circuit controls panel movement and effectively supports IoT-based monitoring. The design of the circuit is illustrated in Figure 3, which shows the electrical schematics on Arduino using the Fritzing application. The technical specifications of the hardware used in this study are summarized in Table 1, while the supporting components, including auxiliary tools and software for system operation and data acquisition, are listed in Table 2.

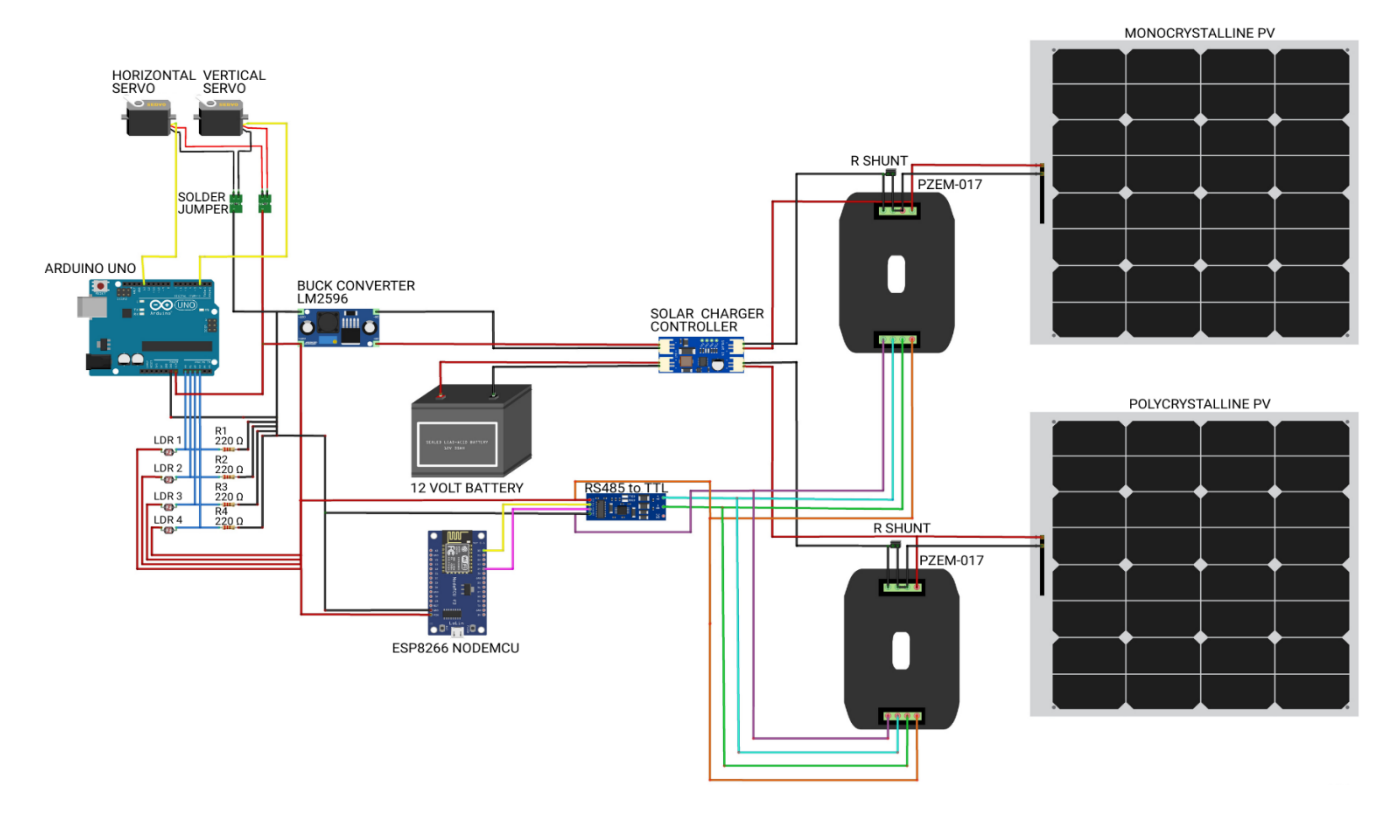


Figure 3. Electrical schematics on Arduino using the fritzing application

Table 1. Technical specifications of the hardware used

Number	Component	Specifications				
1.	Monocrystalline Solar Panel	This monocrystalline solar panel with a half-cell design measures $415 \times 340 \times 30$ mm and weights 320 grams, utilizing monocrystalline silicon cells [19]. With a maximum power output of 18 W, the panel operates at a voltage of 18 V and a current of 1.11 A. Its specifications include Voc 22.2 V and Isc 1.11 A,				
2.	Polycrystalline Solar Panel	making it efficient for light energy needs such as portable devices or outdoor use [20]. This polycrystalline solar panel with a half-cell flexible type with dimensions of $420 \times 280 \times 25$ mm and a lightweight design of only 300 grams, making it portable and easy to install. It uses polycrystalline silicon solar cells and delivers a maximum power output (Pmax) of 18 W. Under standard test conditions (25°C, 1000 W/m²), the panel operates at a maximum power voltage (Vmp) of 17.6 V and a maximum power current (Imp) of 1.13 A. It also has an open-circuit voltage (Voc) of 22.1 V and a short-circuit current (Isc) of 1.24 A, ensuring reliable performance for small-scale energy needs such as portable devices or outdoor applications				

3.	Arduino UNO	This microcontroller is based on the ATMega328 and operates with a supply voltage between 7 to 12 V, while its input voltage range can reach 6 to 20 V. It provides 14 digital I/O pins, including 6 PWM pins, and six analog input pins, making it versatile for various electronic applications. Each I/O pin can handle up to 40 mA of DC, while the 3.3 V pin supports up to 50 mA. The device is equipped with 32 KB of flash memory (with 0.5 KB reserved for the bootloader), 2 KB of SRAM, and 1 KB of EEPROM. Running at a clock speed of 16 Hz, this microcontroller is suitable for lightweight embedded systems and prototyping [3, 5, 22, 23].
4.	Light Dependent Resistor Sensor	This component operates with a supply voltage of 3.3 V to 5 V and has a spectral peak at 540 nm, making it sensitive to green light in the visible spectrum. It is designed to handle a maximum voltage of 150 V and a maximum power of 100 mW, ensuring safe performance under specified limits. The device functions reliably within an operating temperature range of $-30^{\circ}$ C to $+70^{\circ}$ C. Its resistance level varies from 10 $\Omega$ to 100 k $\Omega$ , adapting based on external conditions. At the same time, the response time is 20 seconds for rising and 30 milliseconds for falling, indicating stable yet efficient performance for sensing applications [5, 15, 24].
5.	Servo Motor	This device operates with a voltage range of 4.8 to 6.8 V and offers high precision performance. At 5.0 V, it achieves an operating speed of 0.15 seconds per 60°, while at 6.8 V, the speed improves to 0.13 seconds per 60°. Its stall torque reaches 21 kg·cm at 5.0 V and 25 kg·cm at 6.8 V, providing a strong rotational force. The servo has a dead band of 3 μs and supports a working frequency between 50 to 333 Hz. It comes with a ±300 mm connector wire, uses durable metal gears, and is driven by a DC motor. Compact in design, the unit measures 40 × 20 × 40.5 mm and weighs only 67 grams, making it suitable for robotics and mechanical applications requiring strength and reliability [22].
6.	ESP8266	This development board is based on the ESP-8266 32-bit microcontroller and uses the NodeMCU Amica model (CP2102 version). With compact dimensions of 49 × 26 mm and a pin spacing of 0.9 inches (22.86 mm), it is well-suited for prototyping and IoT applications. The board runs at a clock speed of 80 MHz and integrates a CP2102 USB-to-serial converter with a Micro USB connector for easy programming. It operates at 3.3 V with an input voltage range of 4.5 V to 10 V. Memory resources include 4 MB of flash storage and approximately 80 KB of SRAM, providing sufficient code and data handling. It offers 11 digital I/O pins and 1 analog input channel with a 10-bit ADC supporting a range of 0 to 3.3 V. Designed for robust use, the board functions within a temperature range of –40°C to +125°C, making it reliable for various embedded system and IoT projects [7].
7.	INA219 Sensor	This module operates with a voltage range of 3.0 V to 5.5 V and supports a maximum bus voltage of 26 V DC, making it suitable for low-power monitoring applications. It can measure currents up to $\pm 3.2$ A, depending on the value of the shunt resistor, with a typical accuracy of $\pm 1\%$ . The device provides a fine current measurement resolution of up to 0.1 mA. The device provides a fine current measurement resolution of up to 0.1 mA and a bus voltage resolution of up to 4 mV, ensuring precise monitoring. Communication is handled via the I2C interface, with a default address of 0 × 40, making integration with microcontrollers and
8.	BH1750 Sensor	embedded systems straightforward.  This sensor operates with a voltage range of 2.4 V to 3.6 V and offers selectable resolutions of 1 lux, 0.5 lux, or 4 lux, depending on the chosen mode. It provides a typical measurement accuracy of ±20% and communicates digitally through an I2C interface, allowing easy integration with microcontrollers. During operation, the device consumes only about 0.12 mA, while in standby mode the current drops to around 0.01 μA, making it highly energy - efficient. The typical measurement time is 120 ms in high-resolution mode, ensuring responsive light detection. The sensor is suitable for various environmental and embedded
9.	LM2596 Buck Converter	applications with an operating temperature range from -40°C to +85°C.  This module uses the LM2596 switching regulator IC and is designed to step down DC voltage efficiently. It accepts an input voltage range of 4.5 V to 40 V DC and provides an adjustable output voltage between 1.25 V and 37 V DC, making it versatile for various power supply applications. The module can deliver a maximum output current of 2 to 3 A and operates at a switching frequency of around 150 kHz. An efficiency of up to 92% ensures minimal power loss during voltage conversion. Physically, the board is relatively large
10.	Solar Charger Controller	(approximately 43 × 21 mm), offering stability and heat dissipation for higher current loads. The solar charger controller regulates the flow of electrical current from the solar panels to the battery, preventing overcharging and over-discharging, which can damage the battery. The PZEM-017 is a sensor module from Peacefair used to monitor various electrical parameters in a DC
11.	PZEM-017	system, such as voltage, current, power, and energy. This module is designed to measure voltages up to 300 V DC and currents up to 50 A or more, depending on the type of shunt resistor used. The PZEM-017 is equipped with an RS-485 communication interface based on the Modbus RTU protocol, making it easy to integrate with microcontrollers, PLCs, or computer-based monitoring systems [25]. This module is widely used in solar panel monitoring, battery systems, and various electronics projects requiring accurate and real-time power consumption tracking.

 Table 2. Supporting components

Number	Component	Specifications				
1.	PLX-DAQ	Parallax Data Acquisition (PLX-DAQ) is software that acts as a bridge between microcontrollers, such as Arduino, and Microsoft Excel. Using this software, data from Arduino can be captured and recorded directly into Excel tables in real time. This makes it easy for users to monitor, log, and analyze data without copying or				
		processing it manually. This application is widely used in experimental projects, research, and simple monitoring systems requiring direct computer data logging [23].				
2.	Computer	This computer, identified as Desktop-192718C, is powered by an Intel Core i5-2400 CPU running at 3.10 GHz, providing reliable performance for everyday computing tasks. It is equipped with 8 GB of RAM, which supports multitasking and moderate workloads. The system operates on a 64-bit Windows 10 Pro operating system with an ×64-based processor architecture, ensuring compatibility with modern applications and offering enhanced performance compared to 32-bit systems. This setup is suitable for office work, programming, and general-				
		purpose use.				

Blynk is an application that allows users to control and monitor electronic devices remotely via a smartphone. Blynk Blynk facilitates smartphone integration and microcontrollers such as Arduino, ESP8266, or ESP32. Users can 3. Application create a virtual dashboard to access sensors, control actuators, and monitor data in real-time using an internet connection. The Asus Fonepad 7 is a tablet device powered by an Intel Atom Z2560 dual-core processor running at 1.6 GHz, delivering adequate performance for basic tasks and multimedia use. It comes with 1 GB of RAM and 32 GB of internal storage (ROM), providing space for apps, media, and files, with support for expandable storage via 4. Smartphone microSD. The device runs on Android 4.3 Jelly Bean, which can be upgraded to Android 4.4 KitKat for improved features and system stability. Overall, the Asus Fonepad 7 is designed as a practical and portable device for browsing, entertainment, and everyday mobile computing. A lux meter is a measuring device used to measure light intensity in lux units. This device captures light using a photosensitive sensor (such as a photodiode or LDR) and converts it into a readable digital value. In this study, 5. Lux Meter the lux meter was used to monitor the intensity of sunlight on the surface of solar panels, which can aid in analyzing the relationship between sunlight intensity and the performance of a dual-axis solar tracking system. A multimeter is a measuring device used to measure electrical quantities, including voltage (volt), current (ampere), and resistance (ohm). Multimeters can operate in digital or analog mode, with measurements taken 6. Multimeter using probes connected to the circuit. In this study, a multimeter was used to measure and calibrate a solar panel's voltage and current output.

#### 4. RESULTS AND DISCUSSION

#### 4.1 Experimental results

This research was obtained from testing two types of solar panels, monocrystalline and polycrystalline, equipped with an Arduino based dual-axis solar tracker system [26]. Data collection was carried out over a period of 31 days, starting on July 1, 2025, to July 31, 2025. Measurements included four main variables, namely sunlight intensity (lux), voltage (V), current (I), and power (P) calculated using the Eq. (1).

$$P = V \times I \tag{1}$$

Data was recorded automatically and in real-time with a data collection interval of every 15 minutes from 7:00 AM until 5:00 PM. During the observation process, 1,271 electrical voltage data points, 1,271 electrical current data points for each solar panel, and 1,271 sunlight intensity data points were obtained over the same period. Data was automatically recorded using PLX-DAQ and monitored using the IoT-based Blynk Application.

In general, monocrystalline solar panel performed better than polycrystalline solar panels. Table 3 summarizes the average daily measurement results.

The results in Table 3 show that a monocrystalline solar panel can produce an efficiency of 16.35%, higher than a polycrystalline solar panel, which has an efficiency of 7.11%.

**Table 3.** Average performance of dual-axis solar tracker

Parameter	Monocrystalline	Polycrystalline	Difference
Average Voltage (V)	14.53	14.33	+0.2
Average Current (I)	0.33	0.15	+0.18
Average Power (P)	4.91	2.22	+2.69
Efficiency (%)	16.35	7.11	+9.24

## 4.2 Performance trend over time

Figure 4 shows a graph of sunlight intensity on the dual-axis solar tracker system during the 31 days data collection process. The highest sunlight intensity received by the solar panel was recorded at 88,054.86 lux at 11:15 AM, while the lowest light intensity was 4,911.82 lux at 5:00 PM.

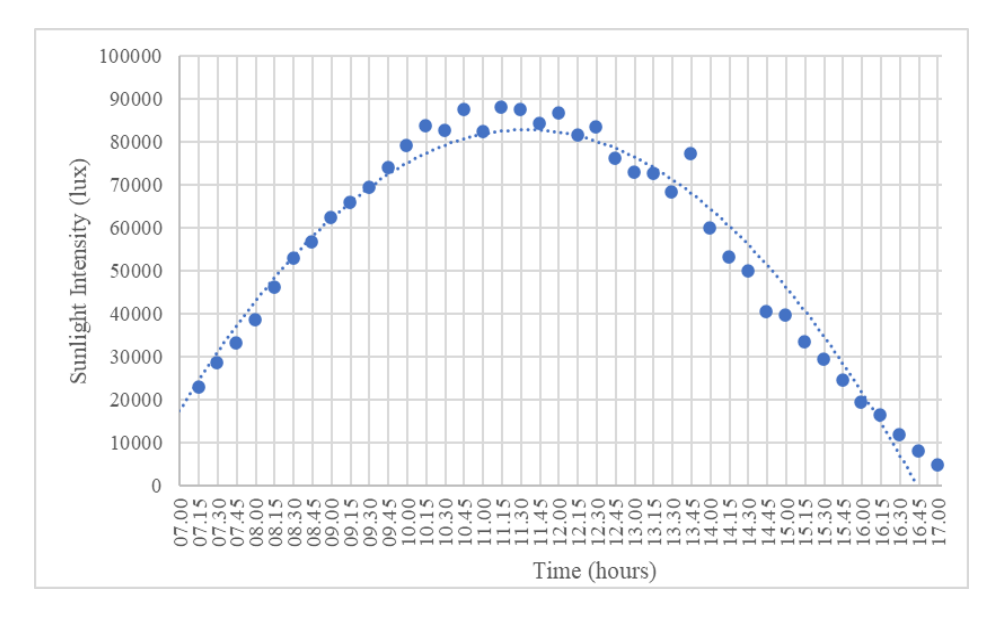


Figure 4. Chart of sunlight intensity on a dual-axis solar tracker system over 31 days

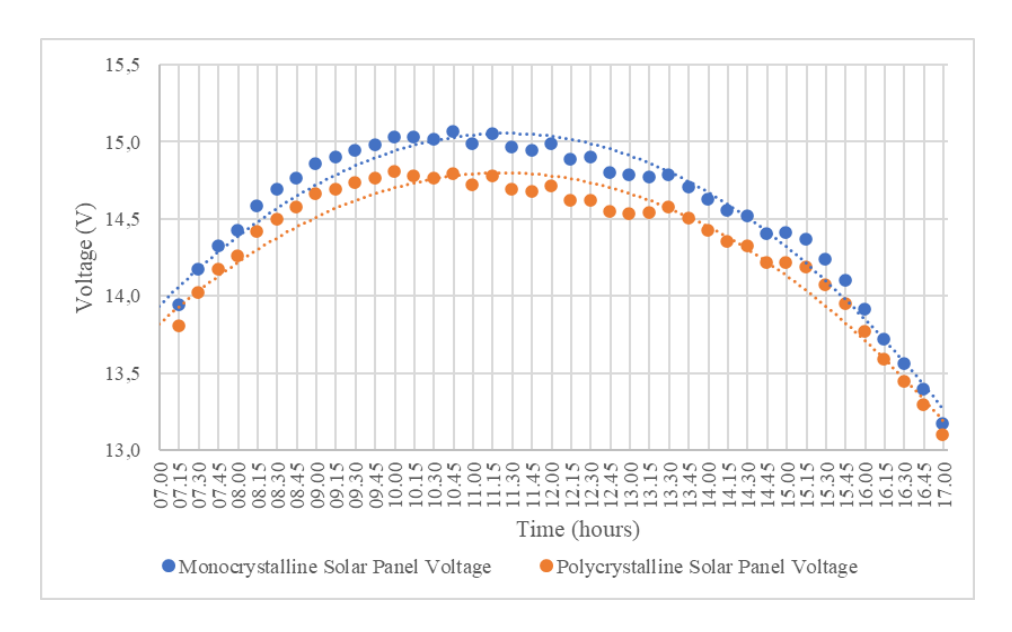


Figure 5. Chart of monocrystalline and polycrystalline solar panel voltage comparison over 31 days

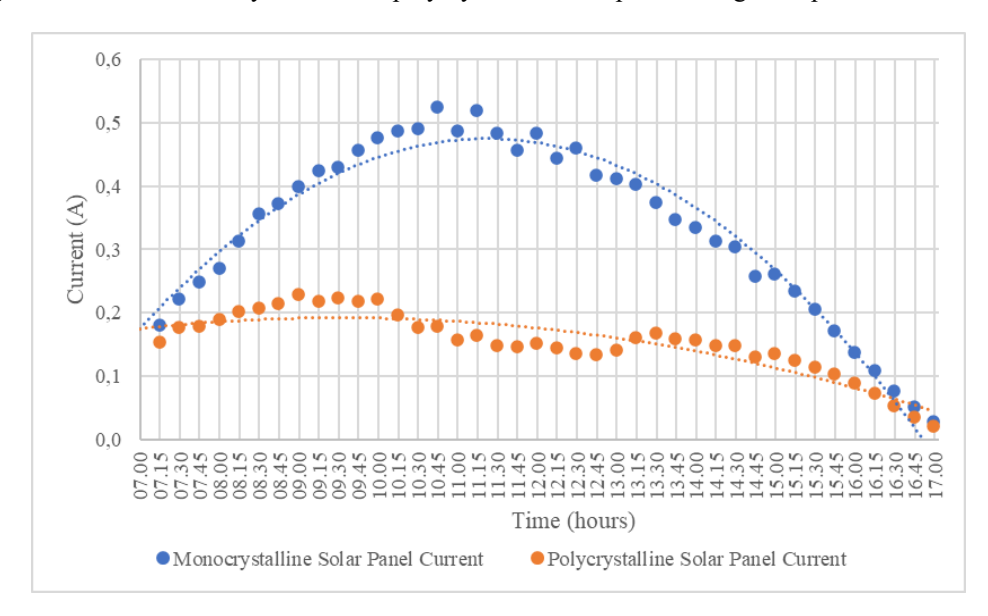


Figure 6. Chart of monocrystalline and polycrystalline solar panel current comparison over 31 days

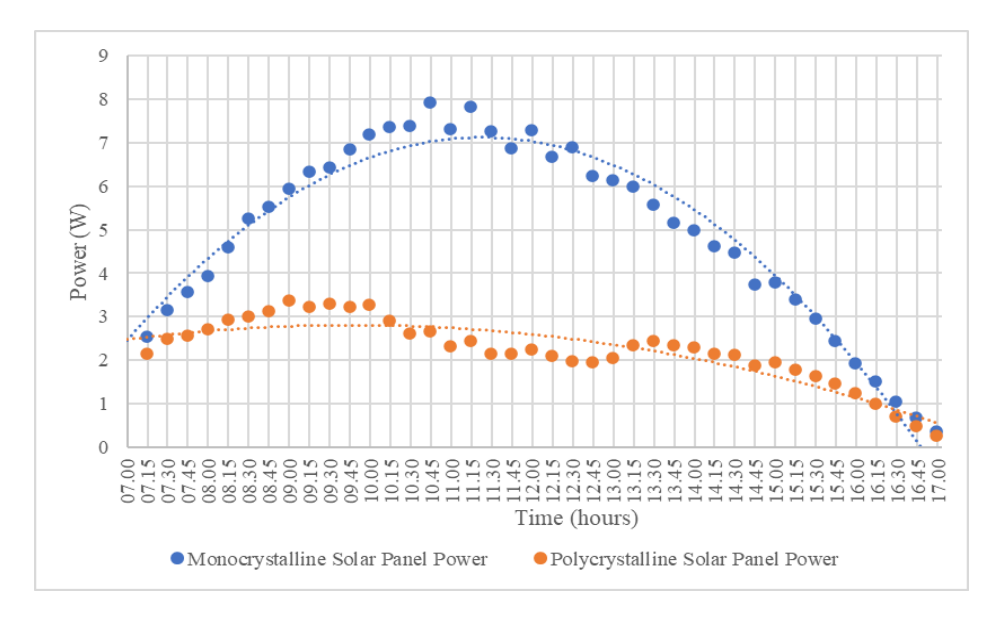


Figure 7. Chart of monocrystalline and polycrystalline solar panel power comparison over 31 days

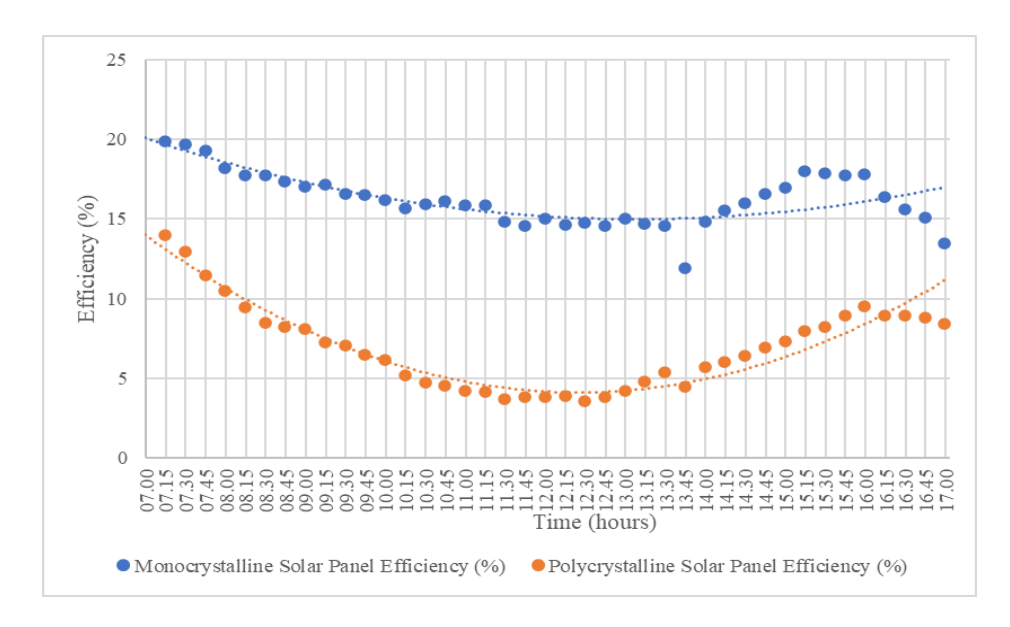


Figure 8. Chart of monocrystalline and polycrystalline solar panel efficiency over 31 days

Figure 5 shows a comparison chart of the electrical voltage produced by the two types of solar panels. From the data obtained, the two types of panels have a difference of 0.2 V from the average data obtained over 31 days. The monocrystalline solar panel has an average voltage of 14.53 V. Meanwhile, the polycrystalline solar panel has an average voltage of 14.33 V.

Figure 6 shows a comparison chart of the current generated by the two types of solar panels. From the data obtained, the two types of panels have a difference of 178 A from the average data obtained over 31 days. The monocrystalline solar panel can generate an average electrical current of 331.1 A over 31 days. Meanwhile, the polycrystalline solar panel can generate an electric current of 153.1 A.

Figure 7 shows a comparison chart of the power generated by the two types of solar panels. From the data obtained, the two types of panels have a difference of 2.69 W from the data obtained over 31 days. Monocrystalline solar panels can generate an average power of 4.91 W over 31 days. Meanwhile, polycrystalline solar panels can generate an average power of 2.22 W over 31 days.

Figure 8 shows a chart comparing the efficiency of the two types of panels. From the data obtained, the two types of panels have a difference of 3.07% from the average data obtained over 31 days. The monocrystalline solar panel has an average efficiency of 8.21%, while the polycrystalline solar panel has an average efficiency of 5.14%.

## 4.3 The effect of temperature on solar panel performance

The results of this study also show that module temperature plays a major role in reducing the efficiency of solar panels. Module temperature is the average temperature on the surface of the solar panel, particularly on the back of the solar panel, which is an important indicator for describing thermal conditions. Based on the research findings, module temperature reached 44.1°C for monocrystalline panels and 45.5°C for polycrystalline panels during the daytime. These conditions cause a decrease in output voltage and affect the reduction in energy conversion efficiency. Conversely, in the morning when module temperature is still within the range of 31.9°C to 42.4°C for monocrystalline panels and 32.1°C to 43.8°C for polycrystalline panels, the efficiency of both solar

panels tends to be higher due to optimal thermal conditions. In the afternoon, the module temperature drops back to a range of 25°C to 32.8°C for monocrystalline panels and 25.9°C to 33.9°C for polycrystalline panels after reaching its peak during the day, so the efficiency of the solar panels also increases and becomes more stable. This finding reinforces that module temperature is one of the factors influencing the daily performance of solar panels, regardless of the intensity of sunlight received.

### 4.4 Effect of sunlight intensity on output

Average sunlight intensity data recorded over 31 days between 7:00 AM and 5:00 PM showed a consistent daily pattern. At 7:00 AM, the sunlight intensity reached 17,781.46 lux. This value continued to increase with the rising sun, peaking at 88,954.86 lux at 11:15 AM. After reaching this peak, the intensity gradually decreases, reaching a minimum value of 4,911.82 lux at 5:00 PM. The average light intensity over the 31 days data collection period is 55,007.97 lux.

# 4.5 Statistical analysis of panel efficiency

Inferential statistical tests were conducted to strengthen the descriptive findings, namely the independent samples T-test and the one-way ANOVA [27]. These tests were applied to evaluate whether the observed efficiency differences between monocrystalline and polycrystalline panels and across different measurement periods (morning, noon, and afternoon) were statistically significant. The independent samples T-test was used to compare the mean efficiencies of the two solar panels. The test was calculated using the following formula:

$$t_0 = \frac{\bar{Y}_1 - \bar{Y}_2}{s_p \sqrt{\frac{1}{n_1} + \frac{1}{n_2}}} \tag{2}$$

Or

$$t_0 = \frac{\bar{Y}_1 - \bar{Y}_2}{\sqrt{\frac{s_1^2}{n_1} + \frac{s_2^2}{n_2}}}$$
(3)

 $Y_1$  and  $Y_2$  are the averages of samples 1 and 2,  $n_1$  and  $n_2$  are the number of data points in samples 1 and 2, and  $s_p$  is the pooled standard deviation, calculated using the Eq. (4):

$$s_p^2 = \frac{(n_1 - 1)s_1^2 + (n_1 - 1)s_2^2}{n_1 + n_2 - 2} \tag{4}$$

Based on 1,271 data collected over 31 days, the resulting T-test was t=17.24 with a significance level of p<0.05. The results prove that monocrystalline panels show higher statistics (16.35%) than polycrystalline panels (7.11%). Following the procedure described by Montgomery [27].

Testing the difference in efficiency of monocrystalline and polycrystalline solar panels was carried out using the one-factor Analysis of Variance (ANOVA) method. In general, the ANOVA test formula is expressed by the F statistic.

$$F_0 = \frac{MS_C}{MS_F} \tag{5}$$

The results of the ANOVA test can be seen in Table 4.

**Table 4.** ANOVA test results for solar panel efficiency (Monocrystalline vs. Polycrystalline)

Source	DF	Adj SS	Adj MS	F- Value	p-value
Treatment	1	1736.1	1736.1	299.3	0.00
Error	80	464.1	5.8		
Total	81	2200.2			

The results of the ANOVA test, as presented in Table 4, show that the treatment factor representing the type of solar panel (monocrystalline and polycrystalline) produced an F-value of 299.3 with a corresponding p-value of 0.00. Since the p-value is far below the significance level of 0.05, the null hypothesis (H0) stating that there is no difference in the mean efficiency between the two types of panels is rejected. This indicates a statistically significant difference in efficiency, with the monocrystalline panel demonstrating a higher average efficiency than the polycrystalline panel.

These results emphasize that while both panels are influenced by diurnal variation in irradiance and temperature, the monocrystalline panel consistently achieves higher performance, validating its superiority under fluctuating tropical conditions.

# 4.6 Discussion

The results of this study are consistent, which confirm that the use of solar trackers can increase electrical energy output compared to static systems [28]. The significant difference in efficiency between monocrystalline and polycrystalline solar panels, which states that monocrystalline solar panel have an advantage in low-light intensity conditions [29].

Average solar radiation data over 31 days shows a consistent daily pattern, with an increase from 17,781.46 lux at 7:00 AM to a peak of 88,054.86 lux at 11:15 AM, then gradually decreasing to 4,911.82 lux at 5:00 PM with an average of 55,007.97 lux. This pattern aligns with the daily movement of the sun and is influenced by atmospheric factors such as cloud cover, which causes small fluctuations. These results support previous findings that sunlight intensity significantly affects energy conversion efficiency in both monocrystalline and polycrystalline solar panels [7, 22]. Furthermore, the developed system demonstrates higher

efficiency by 18.3%, 14.9%, and 10.01% compared to the horizontal configuration, single-axis, and dual-axis solar trackers [16], consistent with the view of that solar panel performance is highly dependent on light intensity and angle of incidence.

The results of the electrical power analysis show that monocrystalline panels perform better than polycrystalline panels, with the highest power reaching 7.91 W at 10:45 AM and a daily average of 4.91 W, while polycrystalline panels only produce a peak power of 3.38 W at 9:00 AM with a daily average of 2.22 W. The power output patterns of both panels follow the trend of solar intensity, although there are differences in peak times. These findings are consistent with, which states that monocrystalline panels are superior under various light intensity conditions, who emphasize the importance of power output and the influence of temperature on solar panel performance [21]. Additionally, the use of a dual-axis solar tracker plays a crucial role in maintaining the panels orientation aligned with the direction of incoming sunlight, thereby enhancing energy absorption efficiency, consistent with the findings [30].

The efficiency of solar panels in this study does not fully follow the pattern of sunlight intensity or the electrical power generated but is influenced by external factors such as panel temperature, environmental conditions, component quality [31]. Monocrystalline panels exhibit higher efficiency with an average of 16.35% and a peak of 21.02% at 7:00 AM, while polycrystalline panels only achieve an average of 7.11% with a peak of 15.25%. This average difference of 9.24% reinforces previous findings that the single-crystal structure of monocrystalline panels is more effective than the multi-crystal structure of polycrystalline panels [29]. High temperatures were found to reduce efficiency, emphasize that climate, panel orientation, and installation quality also influence performance [30, 32]. Furthermore, the use of dualaxis solar tracker plays a crucial role in maintaining the optimal angle for sunlight absorption, ensuring that monocrystalline panels remain superior at high intensities, who reported a 23.21% increase in efficiency and an additional power output of approximately 50 W with a dual-tracker system [30].

Beyond irradiance, several physical and material-related factors may explain the observed efficiency differences. Monocrystalline panels generally have lower temperature coefficients compared to polycrystalline panels, meaning their performance degrades more slowly at higher operating temperatures [33-35]. This characteristic is especially relevant in tropical climates such as Indonesia, where elevated surface temperatures often occur during midday and can significantly impact conversion efficiency. In addition, monocrystalline cells typically exhibit better spectral response, particularly in the infrared region, which allows them to utilize a broader range of the solar spectrum more effectively than polycrystalline cells. These theoretical expectations align with the empirical findings of this study, where monocrystalline modules consistently outperformed polycrystalline ones, both in peak and average efficiency.

Taken together, the results confirm previous empirical studies and support theoretical models of photovoltaic performance. The combination of lower temperature sensitivity, stronger spectral response, and improved angular absorption with dual-axis tracking provides a comprehensive explanation for the superior performance of monocrystalline panels observed in this study.

#### 5. CONCLUSIONS

experimental study of monocrystalline polycrystalline solar panels installed on a dual-axis solar tracker system with IoT-based monitoring shows that the type of panel and tracking mechanism significantly affect performance. The research results indicate monocrystalline solar panels consistently produce higher power output and efficiency compared to polycrystalline solar panels, with average daily efficiencies of 8.21% and 5.14%, respectively, and a maximum efficiency difference of 3.07% during peak sunlight intensity.

The implementation of a dual-axis solar tracker effectively enhances energy output stability by maintaining the panels at an optimal orientation toward sunlight throughout the day. Additionally, the integration of IoT-based monitoring using ESP8266 and the Blynk app, supported by automatic data logging via PLX-DAQ, proved reliable in providing real-time data collection and reducing the potential for human error. These findings suggest that monocrystalline solar panels are more suitable for application in dual-axis solar tracker systems in tropical regions with fluctuating sunlight intensity.

Nevertheless, this study has several limitations. The use of small-scale modules (18 Wp) may not fully represent the performance of higher-capacity photovoltaic systems, and the testing period of only one month does not capture seasonal variations in solar radiation. Moreover, the analysis did not explicitly account for factors such as long-term degradation, dust accumulation, or the impact of partial shading, which may further influence real-world performance.

For future work, it is recommended to scale the system to kilowatt- or megawatt-class installations to evaluate feasibility in large-scale applications, extend the monitoring period to capture inter-seasonal and annual performance variations, and integrate predictive algorithms for intelligent energy management. Further exploration of hybrid approaches, such as solar tracking with cooling systems or machine-learning-based forecasting, may also provide valuable insights for optimizing PV efficiency under diverse climatic conditions.

# ACKNOWLEDGMENT

We sincerely thank to Universitas Sebelas Maret (UNS) for its support of this research through the Research and Community Service Program (LPPM UNS) Indonesia under the contract number 371/UN27.22/PT.01.03/2025.

#### REFERENCES

- [1] Mohamed-Abdulhussein, M., Mohd-Mokhtar, R. (2024). A review of solar tracking configuration and optimization algorithms for the dual axis solar tracker systems. ASEAN Engineering Journal, 14(4): 49-60. https://doi.org/10.11113/aej.V14.20986
- [2] Mpodi, E.K., Tjiparuro, Z., Matsebe, O. (2019). Review of dual axis solar tracking and development of its functional model. Procedia Manufacturing, 35: 580-588. https://doi.org/10.1016/j.promfg.2019.05.082
- [3] Tchao E.T., Asakipaam, S.A., Fiagbe, Y.A.K., Yeboah-Akowuah, B., Ramde, E., Agbemenu, A.S., Kommey, B. (2022). An Implementation of an optimized dual-axis solar tracking algorithm for concentrating solar power plants deployment. Scientific African, 16: e01228.

- https://doi.org/10.1016/j.sciaf.2022.e01228
- [4] Issa, H.A., Abdali, L.M., Alhusseini, H., Velkin, V.I. (2025). Design, modeling, and control of a dual-axis solar tracker using fractional order PID controllers for enhanced energy efficiency. Results in Engineering, 27: 106073. https://doi.org/10.1016/j.rineng.2025.106073
- [5] Pawar, P., Pawale, P., Nagthane, T., Thakre, M., Jangale, N. (2021). Performance enhancement of dual axis solar tracker system for solar panels using proteus ISIS 7.6 software package. Global Transitions Proceedings, 2(2): 455-460. https://doi.org/10.1016/j.gltp.2021.08.049
- [6] Manalu, Y.A., Anisah, S. (2025). Comparative analysis of polycrystalline and monocrystalline solar panels in PV systems. In International Conference on Digital Sciences and Engineering Technology (ICDSET), pp. 288-297.
- [7] Anshory, I., Jamaaluddin, J., Fahruddin, A., Fudholi, A., Radiansah, Y., Subagio, D.G., Utomo, Y.S., Saepudin, A., Rosyid, O.A., Sopian, K. (2024). Monitoring solar heat intensity of dual axis solar tracker control system: New approach. Case Studies in Thermal Engineering, 53: 103791. https://doi.org/10.1016/j.csite.2023.103791
- [8] Pambudi, N.A., Firdaus, R.A., Rizkiana, R., Ulfa, D.K., Salsabila, M.S., Suharno, Sukatiman. (2023). Renewable energy in Indonesia: Current status, potential, and future development. Sustainability, 15: 2342. https://doi.org/10.3390/su15032342
- [9] Nogueira, C.E.C., Bedin, J., Niedzialkoski, R.K., De Souza, S.N.M., Das Neves, J.C.M. (2015). Performance of monocrystalline and polycrystalline solar panels in a water pumping system in Brazil. Renewable and Sustainable Energy Reviews, 51: 1610-1616. https://doi.org/10.1016/j.rser.2015.07.082
- [10] Parida, B., Iniyan, S., Goic, R. (2011). A review of solar photovoltaic technologies. Renewable and Sustainable Energy Reviews, 15(3): 1625-1636. https://doi.org/10.1016/j.rser.2010.11.032
- [11] Wardhani, P.C., Fauziyah, N.A., Fatikasari, A.D., Aryaseta, B., Alfiansyah A.D. (2022). Daily performance profile comparison test of monocrystalline and polycrystalline solar panels. In 3rd International Conference Eco-Innovation in Science, Engineering, and Technology, pp. 131-137. https://doi.org/10.11594/nstp.2022.2721
- [12] Supriyono, T., Omar, G., Tamaldin, N., Soetikno, P., Sumartono, M.R., Romano, A., Yamin, M. (2024). Performance comparison of monocrystalline and polycrystalline photovoltaic modules before testing with a cooling system. Cogent Engineering, 11(1): 2430426. https://doi.org/10.1080/23311916.2024.2430426
- [13] Muthukumar, P., Manikandan, S., Muniraj, R., Jarin, T., Sebi, A. (2023). Energy efficient dual axis solar tracking system using IOT. Measurement: Sensors, 28: 100825. https://doi.org/10.1016/j.measen.2023.100825
- [14] Abdul-Hussein, M.A., Mohammed, J.A.K., Abdul-Lateef, W.E. (2025). Design and implementation of pneumatic actuators in a dual-axis solar tracker under the climatic conditions of Karbala City. Renewable. Energy, 239: 122152. https://doi.org/10.1016/j.renene.2024.122152
- [15] Ponce-Jara, M.A., Pazmino, I., Moreira-Espinoza Á., Gunsha-Morales, A., Rus-Casas, C. (2024). Assessment of single-axis solar tracking system efficiency in equatorial regions: A case study of Manta, Ecuador. Energies, 17(16): 3946.

- https://doi.org/10.3390/en17163946
- [16] Koshkarbay, N., Mekhilef, S., Saymbetov, A., Kuttybay, N., Nurgaliyev, M., Dosymbetova, G., Orynbassar, S., Yershov, E., Kapparova, A., Zholamanov, B., Bolatbek, A. (2024). Adaptive control systems for dual axis tracker using clear sky index and output power forecasting based on ML in overcast weather conditions. Energy and AI, 18: 100432. https://doi.org/10.1016/j.egyai.2024.100432
- [17] Sadeghi, R., Parenti, M., Memme, S., Fossa, M., Morchio, S. (2025). A review and comparative analysis of solar tracking systems. Energies, 18(10): 2553. https://doi.org/10.3390/en18102553
- [18] Vu, H.T.T., Delinchant, B., Ferrari, J., Nguyen, Q.D. (2020). Autonomous electrical system monitoring and control strategies to avoid oversized storage capacity. IOP Conference Series: Earth and Environmental Science, 505: 012045. https://doi.org/10.1088/1755-1315/505/1/012045
- [19] Ong-art, N. (2022). Study and evaluation of energy on the house by standalone photovoltaic systems of half-cell and full cell types. SNRU Journal of Science and Technology, 14(3): 247406. https://doi.org/10.55674/snrujst.v14i3.247406
- [20] Ramful, R., Sowaruth, N. (2022). Low-cost solar tracker to maximize the capture of solar energy in tropical countries. Energy Reports, 8(Supplement 15): 295-302. https://doi.org/10.1016/j.egyr.2022.10.145
- [21] Abo-Zahhad, E.M., Hares, E., Esmail, M.F.C., Salim, M.H. (2024). Simplified modeling of polycrystalline solar module performance in a semi-arid region. Case Studies in Thermal Engineering, 60: 104762. https://doi.org/10.1016/j.csite.2024.104762
- [22] Aigboviosa, A.P., Anthony, A., Claudius, A., Uzairue, S., Timilehin, S., Imafidon, V. (2018). Arduino based solar tracking system for energy improvement of PV solar panel. International Journal for Research in Applied Science & Engineering Technology (IJRASET), 9(VII): 2257-2261. https://doi.org/10.22214/ijraset.2021.36411
- [23] Reddy, N.S., Gowthami, C., Mounika, E., Harshad, S., Kumar, R.V.P. (2022). Real-time data acquisition to excel and monitoring characteristics of solar panel using Arduino. International Journal of Recent Advances in Multidisciplinary Topics, 3(5): 15-20.
- [24] Boukdir, Y., EL Omari, H. (2022). Novel high precision low-cost dual axis sun tracker based on three light sensors. Heliyon, 8(12): e12412. https://doi.org/10.1016/j.heliyon.2022.e12412
- [25] Sujana, I.K., Winarta, A. (2024). Integration of temperature and power data acquisition using Modbus RTU RS485 communication for performance monitoring of thermoelectric cooler box. Journal of Global Engineering Research & Science (J-GERS), 3(1): 7-12. https://doi.org/10.56904/j-gers.v3i1.80
- [26] Liu, X., Song, Y., Xu, Q., Luo, Q., Tian, Y., Dang, C., Wang, H., Chen, M., Xuan, Y., Li, Y., Ding, Y. (2021). Nacre-like ceramics-based phase change composites for concurrent efficient solar-to-thermal conversion and rapid energy storage. Solar Energy Materials and Solar Cells, 230: 111240. https://doi.org/10.1016/j.solmat.2021.111240
- [27] Montgomery, D.C. (2017). Design and Analysis of Experiments. John Wiley & Sons.
- [28] Kumba, K., Upender, P., Buduma, P., Sarkar, M., Simon,

- S.P., Gundu, V. (2024). Solar tracking systems: Advancements, challenges, and future directions: A review. Energy Reports, 12: 3566-3583. https://doi.org/10.1016/j.egyr.2024.09.038
- [29] Taşçioğlu, A., Taşkin, O., Vardar, A. (2016). A power case study for monocrystalline and polycrystalline solar panels in Bursa City, Turkey. International Journal of Photoenergy, 2016(1): 1-7. https://doi.org/10.1155/2016/7324138
- [30] Abd-Elhady, M.M., Agwa, O.M., Bayoumy, M.K., Rizk, R.B., El-Sharkawy, I.I. (2025). Experimental investigation of hybrid photovoltaic-thermal system: Integration of concentration, tracking, and cooling mechanisms. Solar Energy, 299: 113759. https://doi.org/10.1016/j.solener.2025.113759
- [31] Sharaby, M.R., Sharshir, S.W., ElBahloul A.A., Kandeal, A.W., Rashad, M. (2025). Performance evaluation of fixed and sun-tracking photovoltaic systems integrated with spray cooling. Solar Energy, 288: 113310. https://doi.org/10.1016/j.solener.2025.113310
- [32] Moreno, S.A.H., Ramirez, E.R., Bonilla, A.D.L., Contreras, G.G.M., García, B.F.O. (2019). Characterization of a monocrystalline photovoltaic solar panel with cooling to improve its performance. International Journal of Mechanical Engineering and Technology (IJM), 10(11): 297-306.
- [33] Galal, E.M., Abdel-Mawgoud, A.S., Hamed, M.H., Ali, G.A.M. (2023). The performance of polycrystalline and monocrystalline solar modules under the climate conditions of El-Kharga Oasis, New Valley Governorate, Egypt. International Journal of Thin Films Science and Technology, 12(3): 207-215. https://doi.org/10.18576/ijtfst/120306
- [34] Adolf, K., Uzorka, A. (2025). Effects of substrates on the efficiency of a monocrystalline solar panel. Scientific Reports, 15: 6667. https://doi.org/10.1038/s41598-025-90523-0
- [35] Hudişteanu, V.S., Cherecheş, N.C., Țurcanu, F.E., Hudişteanu, I., Romila, C. (2024). Impact of temperature on the efficiency of monocrystalline and polycrystalline photovoltaic panels: A comprehensive experimental analysis for sustainable energy solutions. Sustainability, 16(23): 10566. https://doi.org/10.3390/su162310566

## **NOMENCLATURE**

- V Output voltage of the solar panel, v
- I Output current of the solar panel, A
- P Electrical power output, W
- I<sub>rad</sub> Solar radiation intensity, Wm<sup>2</sup>
- L Light intensity, lx
- A Surface area of the solar panel, m<sup>2</sup>

#### **Greek symbols**

η Solar panel efficiency, %

### **Subscripts**

- In Input values (from solar radiation)
- Out Output values (generated by solar panel)